

# Experimental Analysis of a Single-Flow Double-Channel Solar Air Heater Under Forced and Natural Convection Conditions

E. El-Bialy

Jazan University, College of Science, Department of Physical Sciences/Physics Division, P. O. Box 114, 45142, Jazan, Saudi Arabia

Corresponding Author Email: [i\\_elbially@yahoo.com](mailto:i_elbially@yahoo.com)

[IbrahimAlBili@jazanu.edu.sa](mailto:IbrahimAlBili@jazanu.edu.sa)

**Abstract:** *This study presents an experimental evaluation of a single-flow double-channel solar air heater (SFDC-SAH) tested under both forced and natural convection modes. The SFDC-SAH, designed with two separate air channels and a copper absorber plate, was assessed outdoors for thermal performance across varying air mass flow rates. Results indicate that higher mass flow rates significantly enhance useful heat gain and thermal efficiency, with forced convection achieving up to 2.48 times greater efficiency compared to natural convection. A cost analysis further reveals that forced convection offers the most cost-effective energy output.*

**Keywords:** Solar air heater, Forced convection, Natural convection, Thermal efficiency and Heat gain

## 1. Introduction

The use of solar energy has become an urgent necessity as a renewable energy resource at the present time due to the global decline in the supply of traditional energy resources. A solar air heater (SAH) is one of the thermal applications of solar energy. Over the past decades, many modifications have been made to SAHs to improve their efficiency and overall thermal performance. These attempts include increasing the heat transfer area, as well as creating turbulence in the airflow by adding metal fins embedded in the flow path.

Albdoor, Obaid et al.2024 conducted an experimental study on a SAH implemented with inline and staggered double triangular fins. It is outlined that the daily efficiency as well as annual energy output have been enhanced by about 20.7 and 20.7 %, respectively, compared to the smooth-duct SAH. Many other shapes, geometries and arrangements of fins have been developed for SAHs to improve the thermal as well as thermohydraulic performance over the past few years. These different fin configurations include louvered fins (Chand, Chand et al.2022, Chand, Kumar et al.2024), aerofoil and bio-inspired fins (Vyas, Sharma et al.2024), fins with jet impingement (Almeshaal and Palaniappan 2024), V-shaped aluminum fins (Alrashidi, Altohamy et al.2024), fins of diamond-shaped (Yusaidi, Fauzan et al.2024), rectangular fins with PCM (Balakrishnan, Vishnu et al.2024), spiral fins (Du, Chen et al.2024). The maximum energy efficiency of the SAH using jet impingement fins was found to be 81.4% at Reynolds number = 10850 (Almeshaal and Palaniappan 2024). Moreover, Yusaidi, Fauzan et al.2024 investigated the

impact of different air mass flow rates ranging from 0.0104-0.0261 kg/s on thermal efficiency of the SAH and the highest thermal efficiency of about 59% was experimentally obtained as at mass flow rate = 0.0261 kg/s and solar radiation intensity = 1000 W/m<sup>2</sup>.

This study aims to compare the thermal and economic performance of a single-flow double-channel solar air heater under different convection modes.

## 2. Experimental setup and equipment

A single-flow double-channel SAH (SFDC-SAH) (Fig.1) is designed, manufactured and tested under the weather conditions of Tanta (30° 43'N, 31°E), Egypt during June and July months. The SFDC-SAH has two separate channels; an upper channel and a lower one, separated by an absorber plate (made of 1 mm thick copper), each with its own separate air inlet and outlet. The system is tested in both FCM and NCM on separate days where the FCM is applied from 29 June – 5 July at different values of  $\dot{m}$ , and the NCM is performed on a single day, 6 July. The SFDC-SAH consists of two rectangular flow channels, each 1 m long, 1 m wide, and 0.06 m high, one above and one below the smooth copper absorber plate. Two glass covers are used to ensure minimal overhead heat loss. The system is thermally insulated on the sides and back with a 5 cm thick foam layer to reduce heat loss from the sides and back. The SFDC-SAH is tilted with an angle of 30° (the latitude of Tanta) and faces south to maximize solar radiation throughout the year.

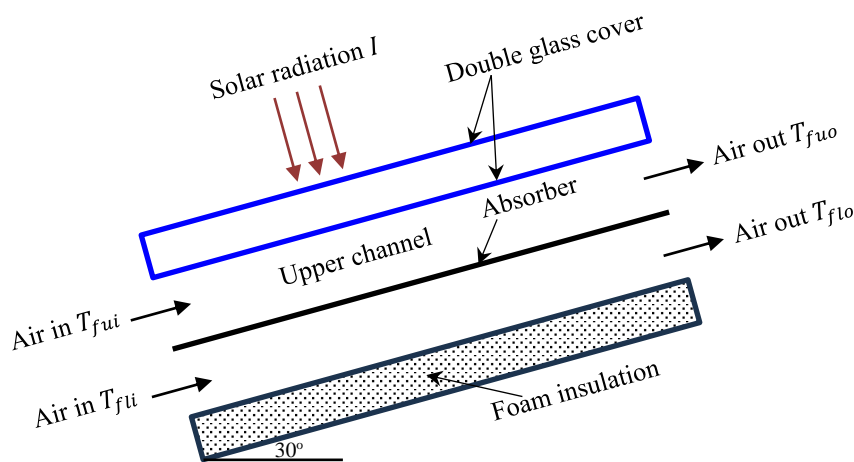


Figure 1: Schematic diagram of the SFDC-SAH.

### 3. Experimental procedure and measurements

During the experiments using FCM,  $\dot{m}$  are controlled using the bypass valve and measured by a laboratory-calibrated orifice gauge. Solar radiation intensity is measured using an Eppley-Precession Spectral Pyranometer connected to a Model No.455 Solar Radiation Meter (0.5% accuracy and 1 W/m<sup>2</sup> resolution). NiCr–Ni thermocouples connected to a Fluke 73 digital multimeter (0.5 °C sensitivity), are used to measure various temperatures for all different SAHs. A High-Pressure Radial Fan 2200 Rpm Brushless DC Centrifugal Blower for Ventilation 178 CFM OEM is used to produce forced airflow. The experiments are conducted under both NCM and FCM to compare which is better: NCM or FCM. The FCM is performed using four values of air  $\dot{m}$  (kg/s); i. e.  $\dot{m} = 0.0105, 0.0118, 0.0131, \text{ and } 0.0157$ .

### 4. Performance Parameters

The instantaneous useful heat gain  $Q_u$  (W) calculated from the experimental data is given by:

$$Q_u = \dot{m} C_f (T_{fo} - T_{fi}) \tag{1}$$

where  $C_f$ : specific heat of air (J/kg K),  $T_{fo}$ : air outlet temperature (K) and  $T_{fi}$ : initial air temperature (K). The daily thermal efficiency  $\eta_{dT}$  can be estimated as:

$$\eta_{dT} = \frac{\dot{m} C_f \Sigma (T_{fo} - T_{fi})}{A_p \Sigma I} \tag{2}$$

## 5. Results and Discussion

### 5.1 Temperature and solar radiation distributions

The SFDC-SAH is studied experimentally using NCM and FCM. The FCM is applied on four days: 29 June, 1, 3 and 5 July with values of  $\dot{m} = 0.0105, 0.0118, 0.0131, \text{ and } 0.0157$  kg/s, respectively, while the NCM is applied on one day, 6 July. Tables 1 and 2 show details of the different measured temperatures for SFDC-SAH operated using FCM (Table 1) and NCM (Table 2) as well as the daily average and total daily solar radiation.

**Table 1:** Different temperatures measured for SFDC-SAH operating under FCM, namely ambient  $T_a$ , hourly average outlet air  $T_{foav}$  and absorber  $T_p$  temperatures as well as the daily average and total daily solar radiation for different days with their corresponding  $\dot{m}$ .

Time of the day	Forced convection mode											
	29 June $\dot{m} = 0.0105$ kg/s			1 July $\dot{m} = 0.0118$ kg/s			3 July $\dot{m} = 0.0131$ kg/s			5 July $\dot{m} = 0.0157$ kg/s		
	Temperature (°C)			Temperature (°C)			Temperature (°C)			Temperature (°C)		
	$T_a$	$T_{foav}$	$T_p$	$T_a$	$T_{foav}$	$T_p$	$T_a$	$T_{foav}$	$T_p$	$T_a$	$T_{foav}$	$T_p$
8	27.0	30.7	35.0	27.6	33.1	35.6	$T_a$	33.7	36.0	28.0	33.6	36.0
9	27.5	35.9	40.5	29.4	40.7	47.4	28.0	39.8	44.0	29.0	36.1	42.0
10	29.0	41.2	52.3	30.5	43.9	51.0	28.5	41.3	48.0	29.7	41.3	47.7
11	29.8	45.7	57.8	31.2	47.4	59.2	29.0	44.4	53.8	32.0	45.1	52.5
12	30.2	50.1	63.2	32.0	51.5	62.5	30.5	47.2	59.0	33.2	48.9	56.5
13	30.8	49.4	58.8	32.9	53.4	65.9	31.0	50.1	59.5	33.0	49.7	58.5
14	32.0	50.4	62.5	33.2	51.7	63.7	31.5	49.8	58.0	33.5	48.8	56.8
15	31.3	48.7	56.8	34.0	51.8	59.5	32.5	47.6	55.8	34.5	47.2	57.8
16	31.0	44.0	51.5	33.7	46.3	54.2	32.5	45.0	50.4	34.5	46.4	52.5
17	30.1	39.8	43.1	33.5	42.1	46.5	32.4	40.7	42.3	34.2	42.1	47.2
18	28.8	36.0	40.0	32.9	38.4	40.9	31.8	36.1	36.1	33.0	38.5	41.0
19	27.7	28.1	33.2	32.5	32.9	38.0	30.6	30.3	29.1	32.0	32.3	32.0
20	26.9	26.9	26.9	32.0	32.0	32.0	29.1	28.8	28.8	30.0	30.0	30.0
Average value (°C)	<b>29.4</b>	<b>40.5</b>	<b>47.8</b>	<b>32.0</b>	<b>43.5</b>	<b>50.5</b>	<b>30.5</b>	<b>41.1</b>	<b>46.2</b>	<b>32.0</b>	<b>41.5</b>	<b>47.0</b>
Average solar radiation (W/m <sup>2</sup> )	<b>600</b>			<b>609</b>			<b>595</b>			<b>576</b>		
Total solar radiation (W/m <sup>2</sup> )	<b>7803</b>			<b>7914</b>			<b>7736</b>			<b>7493</b>		

**Table 2:** Various temperatures measured for SFDC-SAH using NCM, namely  $T_a$ ,  $T_{foav}$  and  $T_p$  as well as the daily average and total daily solar radiation.

Time of the day	Natural convection mode		
	System 1		
	6 July		
	Temperature (°C)		
	$T_a$	$T_{foav}$	$T_p$
8	29.0	29.2	37.0
9	29.8	37.8	47.8
10	29.8	41.8	60.3
11	31.2	48.0	69.5
12	32.0	52.5	80.3
13	33.5	54.0	83.0
14	33.7	52.0	79.2
15	34.0	51.7	77.5
16	35.0	50.6	68.0
17	33.8	43.0	51.8
18	32.8	33.5	43.3
19	32.2	32.3	40.2
20	31.7	32.0	32.5
Average value (°C)	<b>32.2</b>	<b>43.0</b>	<b>59.3</b>
Daily average solar radiation (W/m <sup>2</sup> )	<b>582</b>		
Total daily solar radiation (W/m <sup>2</sup> )	<b>7560</b>		

Figure 2 shows the temperature distribution (i. e.  $T_a$ ,  $T_{foav}$ ,  $T_{gu}$ : upper glass temperature and  $T_p$ ) and incident solar radiation I on a specific day of these five days, 29 June where  $\dot{m} = 0.0105$  kg/s. Figure 8 illustrates the daily average solar radiation incident on System 1 during these five days. From Fig.7, the daily average values of  $T_a$ ,  $T_{foav}$ ,  $T_{gu}$  and  $T_p$  can be obtained as 29.4, 40.5, 35.7 and 47.8 °C, respectively, while the solar radiation reaches its maximum value of 1020 W/m<sup>2</sup> at 1: 00 pm. From the results shown in Fig.8, the daily average solar radiation values are 600, 609, 595, 576 and 582 W/m<sup>2</sup> on 29 June, 1, 3, 5 and 6 July, respectively. The standard deviation of the daily average solar radiation values for the five days of SFDC-SAH experiments under the influence of FCM and NCM is 13.33 W/m<sup>2</sup>. This standard deviation is a reasonable value, and indicates that the variations in the daily average solar radiation over those five days do not significantly affect the performance of SFDC-SAH.

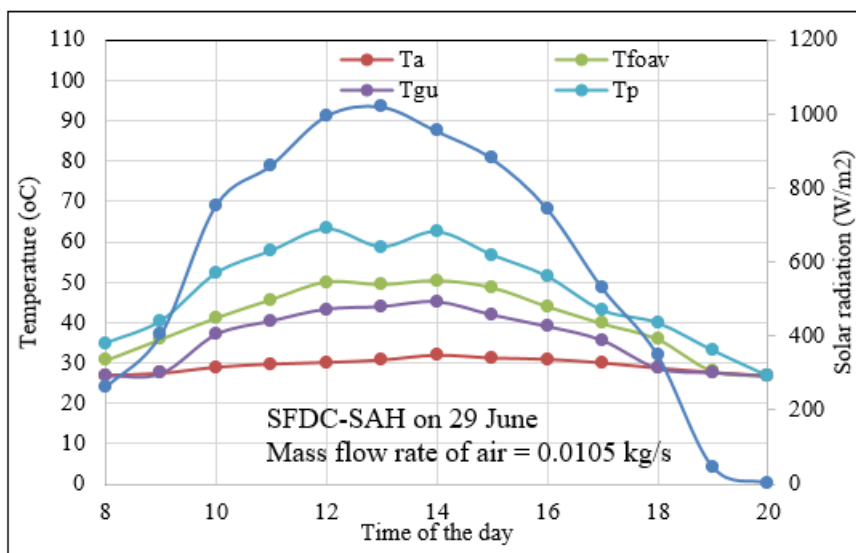


**Figure 2:** Temperature distribution as well as solar radiation incident on SFDC-SAH on 29 June.

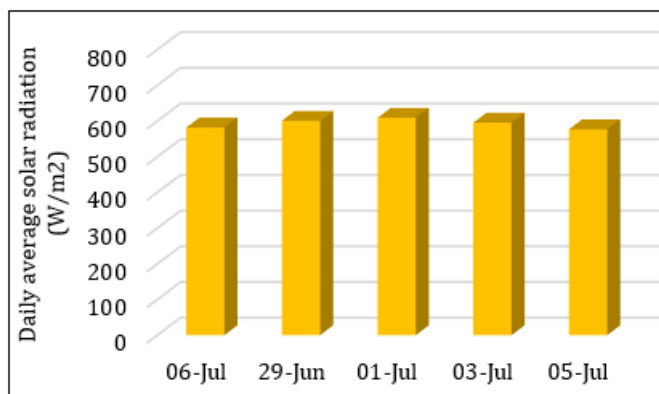


**Figure 3:** Daily average solar radiation incident on SFDC-SAH during five days.

**5.2 Useful heat gain ( $Q_u$ )**

Figure 4 shows variation of the daily average values of useful heat gain  $Q_u$  for SFDC-SAH operating under NCM (6 July)

and FCM (29 June, 1, 3 and 5 July). The useful heat gain  $Q_u$  is calculated using Eq.1 using the measured experimental data. It is clear that daily average values of  $Q_u$  for SFDC-SAH operating under FCM increase with increasing  $\dot{m}$ , which may

be due to the decrease in total heat loss with increasing  $\dot{m}$ . The daily average values of  $Q_u$  are obtained as 61.2, 118.3, 137.6, 141.4, and 150.6 W at NCM,  $\dot{m} = 0.0105, 0.0118, 0.0131$  and  $0.0157$  kg/s, respectively. The daily average value

of  $Q_u$  at  $\dot{m} = 0.0157$  kg/s is maximum and higher than that at  $\dot{m} = 0.0105$  kg/s by 27.36% and superior when NCM is applied by 146.14% because the total heat loss is significant when NCM is applied.

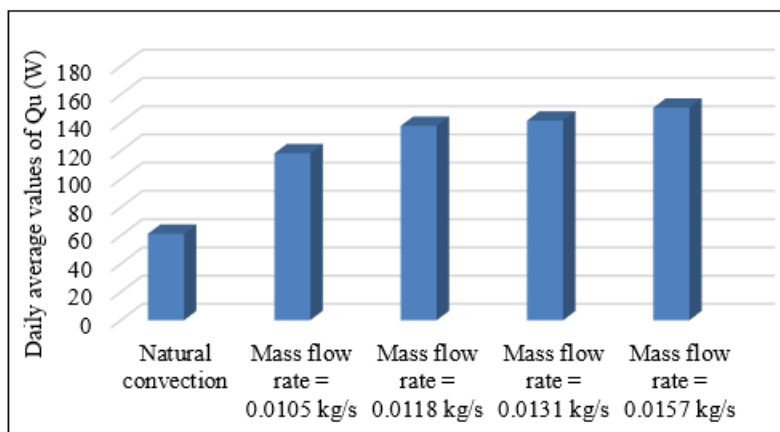


Figure 4: Daily average values of  $Q_u$  for SFDC-SAH operating in both NCM and FCM.

### 5.3 Daily thermal efficiency ( $\eta_{dT}$ )

The variations of daily thermal efficiency  $\eta_{dT}$  of SFDC-SAH operating under NCM and FCM at different  $\dot{m}$  values are illustrated in Fig.5. It is clear from the results shown in Fig.5 that  $\eta_{dT}$  increases with increasing  $\dot{m}$ . The  $\eta_{dT}$  increases as 10.52%, 19.70%, 22.61%, 23.76% and 26.13% at NCM,  $\dot{m} =$

0.0105, 0.0118, 0.0131 and 0.0157 kg/s, respectively. This is mainly because of the increased  $Q_u$  with increasing  $\dot{m}$  (see Fig.4). It is evident that the highest  $\eta_{dT}$  is achieved of  $\eta_{dT} = 26.13\%$  at  $\dot{m} = 0.0157$  kg/s with improvement of 32.63% and 148.34% compared to those of SFDC-SAH at  $\dot{m} = 0.0105$  kg/s and NCM (due to lower  $Q_u$ ; see Fig.4), respectively.

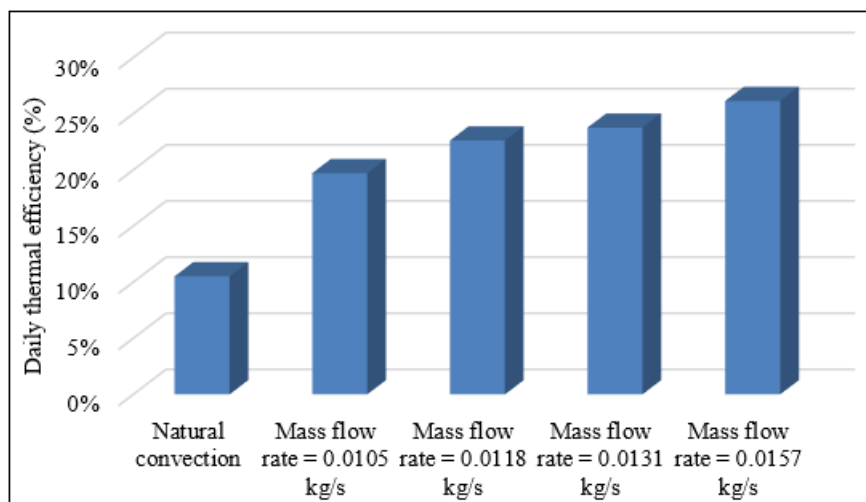


Figure 5: Variations of  $\eta_{dT}$  for SFDC-SAH operated under NCM and FCM.

### Economic analysis

There are two different types of costs for SAHs; i. e., fixed and variable costs. Fixed cost includes absorber plate, back plate, transparent covers, wooden frame, the stand, air blower, etc. Variable cost involves operating hours, maintenance, etc. The governing equations for the cost analysis are presented in Ref. (El-Bialy and Shalaby 2023). The various parameters of the cost study and some results are shown in Table 3. It can be concluded that SFDC-SAH operating with FCM has the best cost per unit energy (CPE), where CPE = 0.03247 \$/kWh, followed by SFDC-SAH using the NCM with CPE = 0.05736 \$/kWh.

Table 3: Some details of cost analysis for the SAHs under study.

Different parameters	SFDC-SAH (NCM)	SFDC – SAH (FCM)
Total IC (\$)	76	106
$Q_u$ (kW)	0.06120	0.15060
$E$ (kWh/year)	229.867	565.654
<b>CPE (\$/kWh)</b>	<b>0.05736</b>	<b>0.03247</b>

### 6. Conclusion

In this work, a single-flow double-channel solar air heater (SFDC-SAH) is designed, manufactured and tested in the summer months of June and July. The SFDC-SAH is tested under both forced (FCM) and natural (NCM) convection modes. The SFDC-SAH with FCM at  $\dot{m} = 0.0157$  kg/s is

more efficient compared to natural convection; as expected, by 2.46 times (with respect to useful heat gain  $Q_u$ ) and 2.48 times (with respect to daily thermal efficiency  $\eta_{AT}$ ). Based on the cost analysis, SFDC-SAH operating with FCM has the best cost per unit energy (CPE), at CPE = 0.03247 \$/kWh, followed by SFDC-SAH using the NCM of CPE = 0.05736 \$/kWh. This investigation provides valuable insights for optimizing solar air heater design for cost-effective energy solutions, particularly in regions with high solar potential. Moreover, this work confirms that operating a single-flow double-channel solar air heater under forced convection significantly boosts thermal performance and cost-efficiency compared to natural convection. The results advocate for the broader application of forced convection systems in solar energy utilization.

## References

- [1] Albdoor, A. K., et al. (2024). "Energy, exergy, economic and environmental analysis of a solar air heater integrated with double triangular fins: Experimental investigation. " *International Journal of Thermofluids* **24**: 100979.
- [2] Almeshaal, M. and M. Palaniappan (2024). "Assessment and enhancement of thermal performance for ring roughened finned jet impingement solar air heater for low-temperature applications. " *Energy* **307**: 132632.
- [3] Alrashidi, A., et al. (2024). "Energy and exergy experimental analysis for innovative finned plate solar air heater. " *Case Studies in Thermal Engineering* **59**: 104570.
- [4] Balakrishnan, P., et al. (2024). "Experimental thermal performance of a solar air heater with rectangular fins and phase change material. " *Journal of Energy Storage* **84**: 110781.
- [5] Chand, S., et al. (2022). "Thermal performance enhancement of solar air heater using louvered fins collector. " *Solar Energy* **239**: 10-24.
- [6] Chand, S., et al. (2024). "Impact of collector aspect ratio on the energy and exergy efficiency of a louvered fin solar air heater. " *Case Studies in Thermal Engineering* **63**: 105312.
- [7] Du, J., et al. (2024). "Turbulent flow-thermal-thermodynamic characteristics of a solar air heater with spiral fins. " *International Journal of Heat and Mass Transfer* **226**: 125434.
- [8] El-Bialy, E. and S. Shalaby (2023). "Recent developments and cost analysis of different configurations of the solar air heaters. " *Solar Energy* **265**: 112091.
- [9] Vyas, S., et al. (2024). "Double pass solar air heater with aerofoil and bio-inspired fins: A numerical analysis of thermohydraulic performance. " *Energy* **311**: 133320.
- [10] Yusaidi, N. J., et al. (2024). "Theoretical and experimental investigations on the effect of double pass solar air heater with staggered-diamond shaped fins arrangement. " *Case Studies in Thermal Engineering* **60**: 104619.